Combination of X-ray synchrotron radiation techniques to gather information for clinicians

Solenn Reguer, Cristian Mocuta, Dominique Thiaudière, Michel Daudon, Dominique Bazin

X-ray synchrotron radiation techniques combination to gather information for the clinician.

Solenn Reguer1*, Cristian Mocuta1, Dominique Thiaudière1, Michel Daudon2, Dominique Bazin3

1 Synchrotron SOLEIL, L'Orme des Merisiers, Saint-Aubin - BP 48, 91192 Gif-sur-Yvette, France
2 Service d'Explorations Fonctionnelles, AP-HP, Hôpital Tenon, 4 rue de la Chine, F-75020 Paris, France
3 CNRS–LCMCP–UPMC, Collège de France, 11, place Marcellin-Berthelot, 75005 Paris cedex, France

* *Corresponding author:* solenn.reguer@synchrotron-soleil.fr, tel 01 69 35 97 27

Abstract
Among the different techniques specific to synchrotron radiation, the combination of X-ray absorption spectroscopy with X-ray scattering experiments is a powerful tool to characterize samples with a capability to gather structural and electronic information at the cellular level. In the present contribution, selected examples making use of such techniques, point out as well the information that one can have access to. Via the presentation of the physicochemical data, this paper focuses on displaying the information that has a significant clinical character.

Keywords
Nephrolithiasis, arthritis, osteoporosis, X-ray fluorescence spectroscopy, X-ray scattering, X-ray absorption spectroscopy.

1. Introduction

The possibility to obtain complementary information such as crystalline structure, elemental composition and chemical speciation using non-destructive techniques is a necessary requirement for the research with medical investigation as metal alloys and prostheses, elasticity and probes, trace elements and nephrotoxicity. Indeed, the samples studied, coming from human bodies' specimens, are precious, volume limited and complex. They often present a heterogeneous distribution of the chemical elements. In addition the morphology and structure of the crystallites (or amorphous compounds) constituting the samples are supposed to be pathology dependent. The most important objective implies to determine the local environment of specific chemical elements, and particularly metal ions, in such biological compounds. This is however generally a difficult task. The measurements have to be done at micrometric scale to determine both local order and elemental distribution in the samples studied.

The purpose of the present short review is to describe the opportunities given to the medical community by the use of X-ray synchrotron radiation techniques. The intent is not to provide a comprehensive summary of all the work described in the literature but to give to the clinician useful information by concentrating on particular studies using synchrotron radiation. The examples presented in this paper were mostly performed at DiffAbs beamline, implemented at SOLEIL synchrotron (France). This beamline led to numerous major scientific breakthroughs in materials sciences thanks to the available almost simultaneous combination of following techniques: X-Ray Diffraction (XRD), X-Ray Fluorescence (XRF) and X-ray Absorption Spectroscopies (XAS). As an aid toward a better description of the sample, the combination between XRD, XRF and XAS is of primary importance in the case of pathological calcifications in which it is thus possible to assess the environment of trace element and get a precise structural description of the calcification. In addition, the possible access to a local probe (about few μm) allows to determine the distribution of the characterized compounds on the studied materials.

After a brief description of the DiffAbs beamline, recent results obtained on different kinds of biological entities including pathological calcifications will be presented [1,2]. Of noticed, the very first set of data collected on the SOLEIL Synchrotron was on the DiffAbs beamline and from kidney stone samples [3,4].

2. The DiffAbs beamline

At SOLEIL Synchrotron, the DiffAbs beamline is located on a bending magnet. The permanent magnetic field of 1.71 Tesla yields to a critical energy of 8.6 keV and the horizontal angular aperture is 6 mrad. The beamline provides a monochromatic X-ray beam, tunable in the 3-23 keV energy range and can presently operate in two modes detailed hereafter: the standard beam mode obtained with the main optics and the microbeam mode by adding a secondary focusing optics. The main optical system includes a monochromator located between two long mirrors (50 nm Rh coated Si). The use of these two mirrors that collimate and focus the beam in the vertical plane results in a high rate of harmonic rejection and an increase of the energy resolution. The fixed-exit double crystal monochromator is composed of two independent Si(111) crystals. The first crystal, that is flat, allows the monochromatisation of the incident beam by setting the incident angle and thus selecting only the X-ray energy for which Bragg law is fulfilled. The second crystal, that is mechanical bendable, restores the parallelism between the incoming and outgoing beam and provides a sagittal focusing (in the horizontal plane) of the monochromatic beam. This main optical set

up allow to obtain a monochromatic beam size less than 300 x 300 μm^2 (H x V, Full Width Half Maximum) at the sample position, with a photon flux about $10^{12} – 10^{13}$ $ph.s^{-1}$.

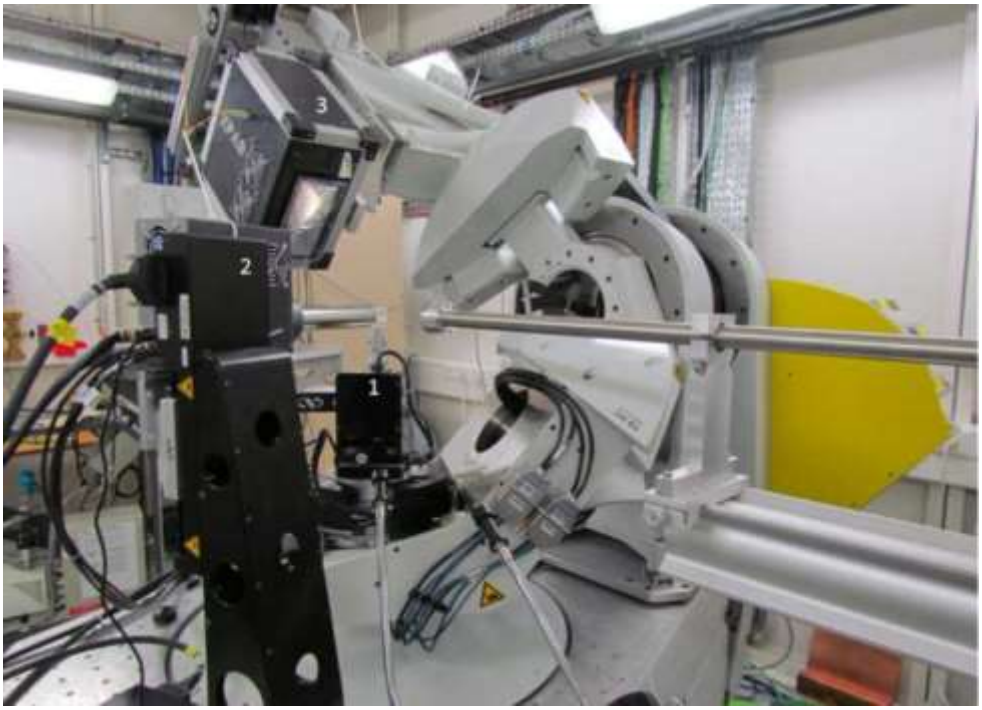

Figure 1: the 6+2 circles diffractometer in Kappa Geometry on DiffAbs beamline with (1) sample positioning using micrometric motorized tables, (2) SDD-4E detector for XRF measurements, (3) hybrid pixel area detector XPAD for XRD measurements.

The secondary optical system consists of two trapezoidal shapes orthogonally placed curved mirrors (Rh coated) under grazing incidence (in Kirkpatrick Baez geometry): each of them is focusing the X-ray beam in one direction. The beam size obtained at the sample position is about 5 x 5 μm^2 (H x V, FWHM) with a flux close to 1010 $ph.s^{-1}$. Apart the obtained small and intense X-ray spot, one of the great advantages of using KB focusing optics is their achromaticity, making them the optics of choice for laterally resolved spectroscopic experiments, in particular EXAFS (Extended X-Ray Absorption Fine Structure) measurements. The applications presented in the present paper and performed at DiffAbs were mainly realized using the microbeam set up. The main experimental instrument on DiffAbs is a 6+2 circle diffractometer (figure 1). This high mechanical precision instrument offers an exceptional potential for all experiments on the beamline.

The diffractometer consists on a goniometric system with 4 circles in the Kappa geometry for the sample orientation and a goniometric system with 2 circles, concentric with the first one, for detector positioning in the vertical and horizontal planes. This geometry corrects and improves the mechanical performance and leaves a large free volume for heavy and bulky sample environments. In addition, a motorized table for the sample position in the X-ray beam and a microscope allow adjusting the sample on the diffractometer and performing X-ray imaging.

Making use of the elastic scattering and the absorption processes, several synchrotron analysis techniques based on XRD or XAS and XRF spectroscopies are available on the beamline (Wide Angle X-ray Scattering, Reflectivity, Anomalous Scattering, Diffraction Anomalous Fine Structure …). All the measurements are performed on the diffractometer using different and well-adapted detectors. Moreover, all these techniques can be used in the

all 3 - 23 keV energy range for both standard and micro beam modes and with various sample environments. This originality makes the beamline of choice to study of a large variety of materials as illustrate by many different topics [5-7]. In addition the coupling of XRD, XAS and XRF spectroscopies is available to correlate the information in the same experimental condition. It means the same X-ray spot position on the sample and thus the possibility to analyze the same area of the sample under the same physico-chemical conditions.

From XAS measurements, it is possible to determine the local order, that is the environment of the probed atoms (geometry, distance of neighbors, speciation). By XRD long range order is accessible, allowing for example the determination of the crystallized phases, the orientation, and other characteristics of crystals. The combination with the microbeam scale and XRF measurements allows a good description of the structure and distribution of the different compounds constituting the samples studied.

Thanks to these characteristics, the DiffAbs beamline is thus well adapted for a great part of biological samples, though no direct access to sub-cell lateral resolution, but it gives a lateral resolution good enough for a lot of studies. Thus, it is possible to analyses very small amount of material, which is interesting when sampling is limited. In addition the concentration of the chemical element measured can be very low, about few hundred part per million (ppm).

3. Shedding light on arthritis

As underlined by Breedveld [8], osteoarthritis, the most known form of arthritis is common in the elderly but also affects younger people. In France during the early 1990s, 6 million new cases were reported each year [9,10] in line with the fact that worldwide 25% of adults aged over 65 years suffer from pain and disability associated with this disease. Its prevalence is expected to increase with the concomitant prevalence of obesity and aging [11]. Osteoarthritis is regarded as a complex disease whose cause is not completely understood and leads ultimately to chronic pain, restriction of joint mobility, and disability. Characterized by articular cartilage, significant modifications are also observed in other joint components including bone, menisci, synovia, ligaments, capsule, and muscles [12].

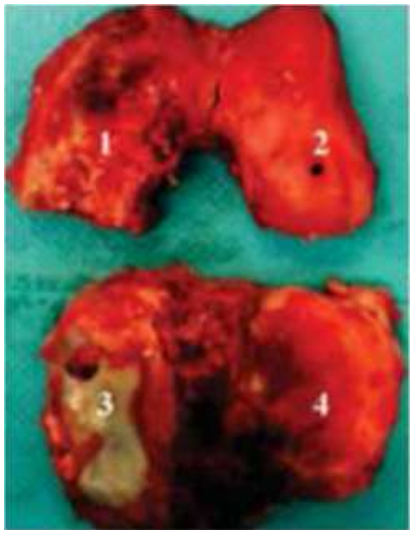

Figure 2: Knee joint specimen obtained during arthroplasty. The specimen included femoral condyle and tibial plateau cartilage from both the medial and the lateral compartments. Cartilage areas were labelled as follows: (1) medial condyle; (2) lateral condyle; (3) medial tibial plateau; (4) lateral tibial plateau.

Through a panel of physicochemical techniques, among others, XAS and XRD performed on DiffAbs and using the microbeam set up, the calcification process which involves several mechanisms was studied [13-17]. Samples correspond to knee joint specimen obtained during arthroplasty (figure 2).

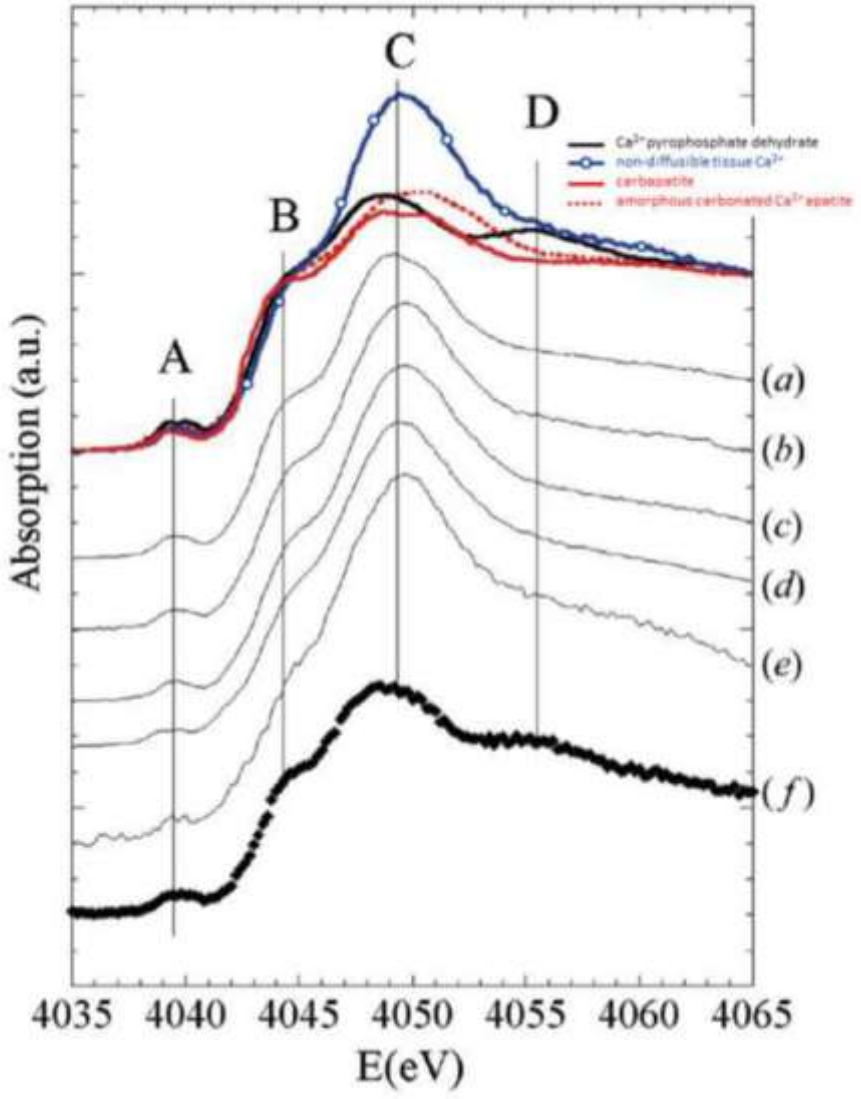

Figure 3: XANES spectra at Ca K-edge obtained on human osteoarthritic articular cartilage compounds and compared to carbapatite (red solid line), amorphous carbonated Ca^{2+} apatite (red dotted line), Ca^{2+} pyrophosphate dehydrate (black solid line) and non-diffusible tissue Ca^{2+} (blue solid line with circles). The (a) to (f) spectra correspond to measures on samples from patients. On theses XANES spectra, the A to D positions correspond to specific features explained in the text.

The samples were firstly analyzed through XAS at the Ca K-edge. The XANES (X-ray Absorption Near Edge Structure) spectra of these samples are compared to references on figure 3. A pre peak (labelled A) is attributed to the 1s to 3d transition and O-2p molecular orbital, an intense resonance corresponding to the 1s to 4p transition, and named the white line, is observed (labelled C). This structure includes a shoulder-like feature (labelled B) corresponding to the 1s to 4s transition. These XANES data support the fact that Ca^{2+}

compounds differ between calcified and non-calcified cartilage areas. In calcified areas they appear to be mainly involved in calcifications. The fact that Ca^{2+} cations are involved in crucial cellular process, and that cartilages are not vascularized, leads to the fact that the number of free Ca^{2+} is drastically decreased locally when calcifications are present in the articulation.

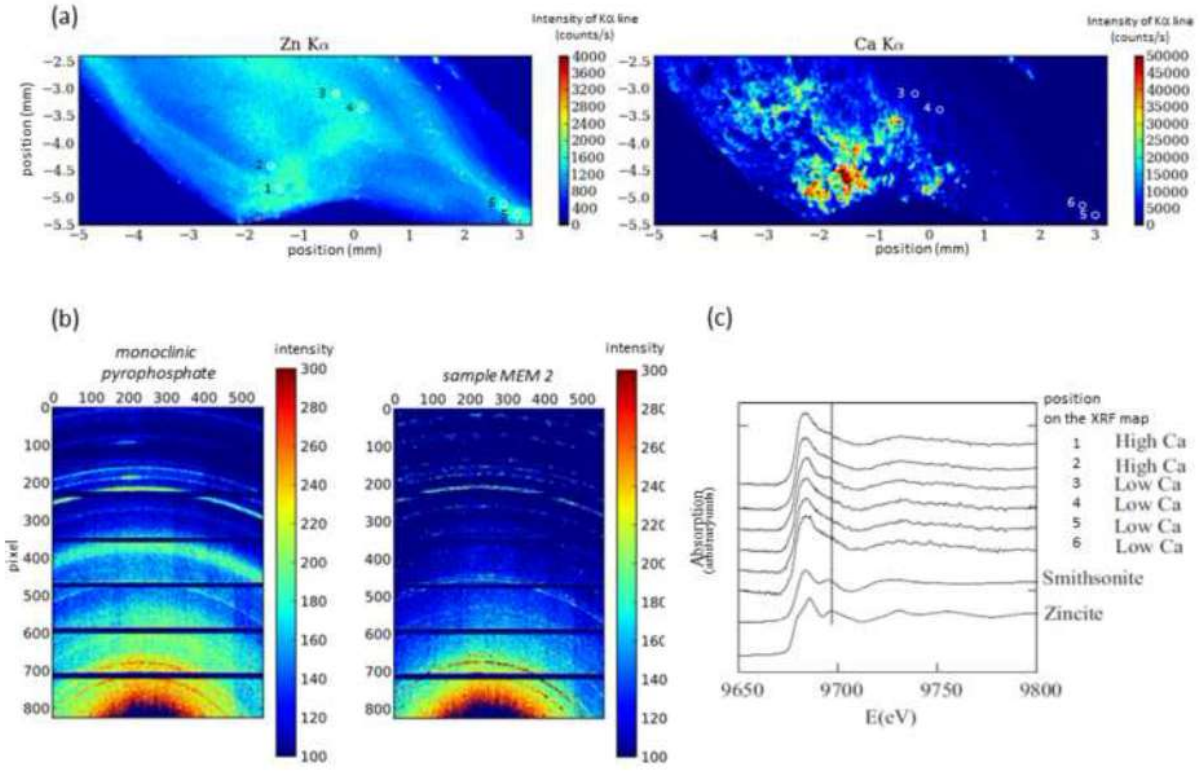

Figure 4: (a) μXRF maps showing Zn and Ca distribution in human cartilage (sample MEM2) with points of interest (b) μXRD image using the XPAD3.2 detector on the sample MEM2 compared to a reference compound (monoclinic pyrophosphate) (c) XANES spectra obtained on the points of interest (from 1 to 6, also noted on the maps) for the sample MEM2.

In addition, the samples were analyzed by combination of XRF, XRD and XAS at Zn K-edge (figure 4). The aim was to evaluate the possible Zn accumulation close to pathological calcifications. These measurements allowed to correlate the distribution (specially Ca and Zn, figure 4a) obtained by XRF map with the structure of the compounds in presence determined by XRD (pyrophosphate, figure 4b) and XAS realized on some points of interest (figure 4c). Different Zn^{2+} species are present in calcified cartilage. It seems that part of Zn^{2+} is trapped in or at the surface of the calcification made of pyrophosphate. Thus, calcifications present in osteoarthritis cartilage may alter the associated biological function of Zn^{2+} metalloproteins.

4. Nephrolithiasis described by XANES investigations

The relationship between vitamin D, Randall's plaque and nephrolithiasis is nowadays still debated [18]. Indeed, Randall's plaque, which serves as a nucleus of kidney stone, constitutes a major public health problem since a dramatic increase in the prevalence of kidney stone developed from a Randall's plaque is observed in western countries [19-21]. In 2010, more than 55% of calcium oxalate (CaOx) kidney stone display a Randall's plaque at their surface in young stone formers aged 20 to 30 years instead of 16% in the 1990s [22-24].

In order to determine locally (from several 10 to 100 µm scale) the structure of phases constituting such Randall's plaque, the environment of Ca was investigated [25].

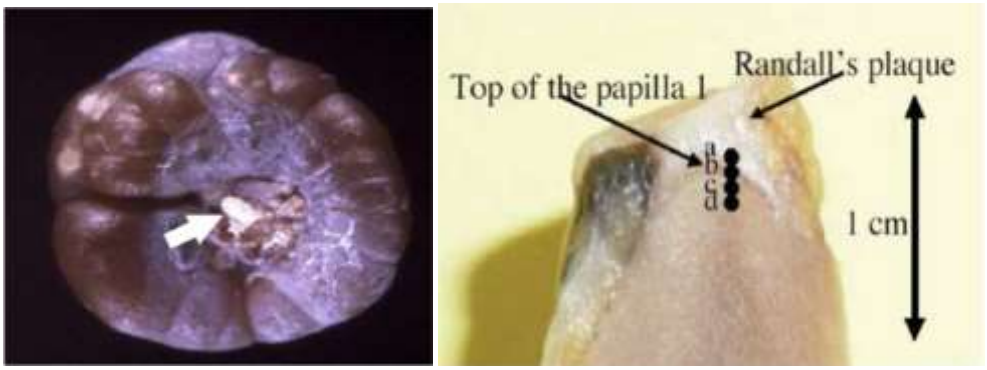

(a) (b)

Figure 5: studied samples: (a) Randall's plaque (white deposit) at the surface of kidney stone (b) Randall's plaque (white deposit) at the surface of a papilla.

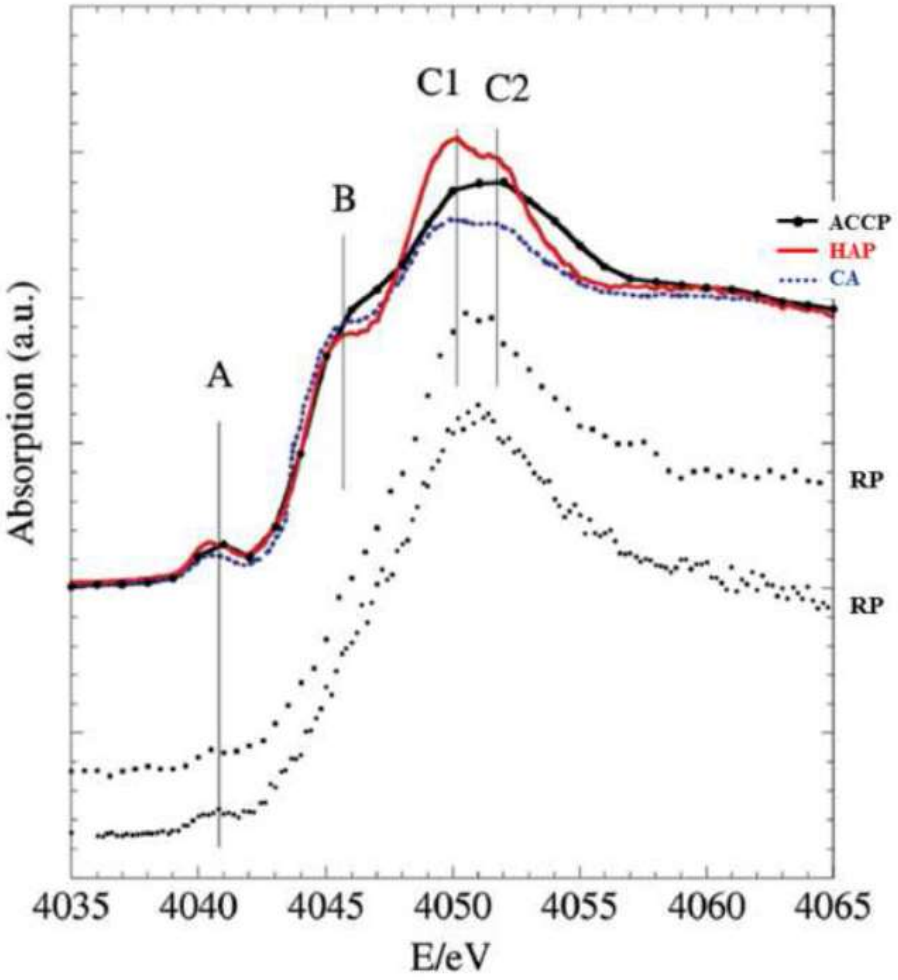

Figure 6: XANES spectra at the Ca K-edge of two Randall's plaque (RP, dot lines) is compared to reference compounds; synthetic well crystallized stoichiometric Ca phosphate apatite (HAP, red), crystallized biological Ca phosphate apatite (CA, blue dots) exhibiting nm size crystals, amorphous carbonated calcium phosphate (ACCP, black with circles).

The studied papillae came from two different kidneys at Nice Hospital after nephrectomy for tumor (figure 5). The XAS spectra, performed at Ca K-edge on DiffAbs beamline and using the microbeam set up, are presented on figure 6 and compared to references as biological apatite (CA for Carbapatite) and its precursor (ACCP for Amorphous Carbonated Calcium Phosphate). As from previous example, specific features describe the spectra. While the feature A is quite the same in the biological apatite (CA) and its precursor (ACCP), significant variations are measured for the shoulder B as well as for the double peak at the maximum of the white line (labelled C1 and C2). Such significant differences allow us to describe precisely the environment of Ca even if the sample is hydrated.

The XANES results suggest that Randall's plaque is composed mainly of ACCP and not of CA. ACCP is evidence of an oversaturation in calcium phosphate by an excess of calcium and/or phosphate and/or due to a too high pH. Its presence in increasingly young subjects raises the question: does nutrient-enriched food specially aimed at young children affect the physiology of the kidney? The debate is still open.

5. Osteoporosis and strontium ranelate, the local environment of Sr^{2+}

Osteoporosis, characterized by an increase in bone fragility due to low bone mass and deterioration of bone quality affects an estimated 75 million people in Europe, USA and Japan corresponding to more than 8.9 million fractures annually [26]. The public health burden of osteoporotic fractures will rise in future generations, due in part to an increase in life expectancy. Recently, Strontium-drug has been introduced as a pharmacological agent for the treatment and prevention of osteoporosis and has shown anti-fracture efficacy in the treatment of postmenopausal osteoporosis [27-29]. Different techniques have been used to assess the localization of Sr^{2+} cations in human bones. For example, Rossi *et al.* [30] have collected electron energy loss near edge structures from P, C, Ca and Sr and showed physicochemical modifications in the bone mineral at the nanoscale caused by the systemic administration of strontium ranelate. In order to observe mineralization changes, Busse *et al.* [31] have performed quantitative backscattered electron imaging and energy-dispersive X-ray analyses combined with micro-XRF. The complete study suggests that strontium ranelate might be considered as a therapeutic option for patients following long-term bisphosphonate treatment. Proton induced X-ray emission (PIXE) method can be also used for the determination of elemental concentrations in femoral heads [32]. More recently, Wohl *et al.* [33] have evaluated the accumulation of strontium in bones through in vivo XRF in rats supplemented with strontium citrate and strontium ranelate. Scattering techniques can be used but as underlined in a recent publication [34], these techniques [35-38] are sensitive to Sr content within the mineral crystals but ignore other types of noncrystalline strontium deposits.

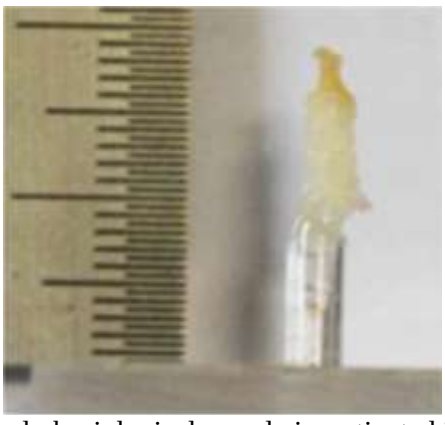

Figure 7: Illustration of the typical physiological sample investigated in this study

Several academic researches [39-43] have evaluated the modifications of the crystal size during the insertion of Sr^{2+} cations in apatite. Bigi *et al.* [41] and Suganthi *et al.* [43] found very different results regarding the effect of Sr^{2+} on the crystallinity and the crystallite size of hydroxyapatite (HAP). In fact, the complete set of such studies indicates clearly that the insertion of Sr^{2+} cations in apatite is a complex process which is very sensitive to preparation methods. Structural investigation through XAS has also been performed [44-50]. The local environment of Sr^{2+} cations in biological apatites (figure 7) present in pathological and physiological calcifications in patients without such Sr-based drugs was assessed through XAS experiments on DiffAbs [51-52].

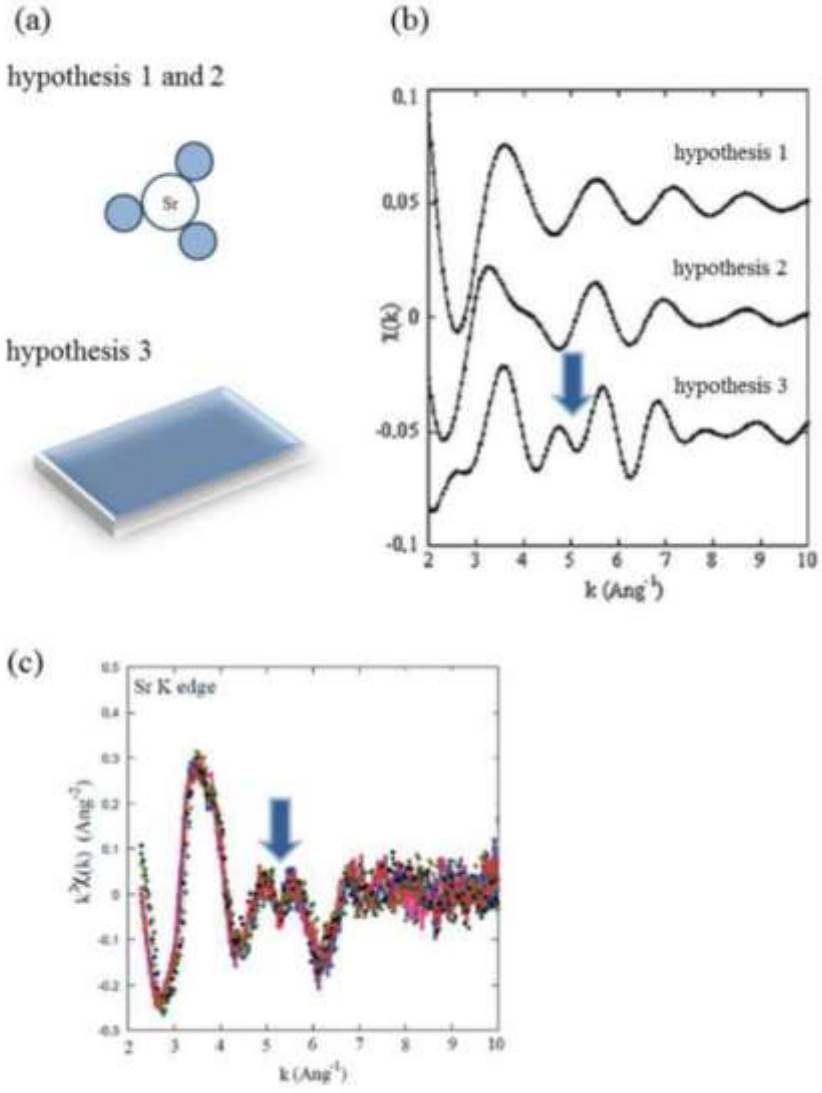

Figure 8: (a) Three different structural hypothesis regarding the adsorption at the surface of Ca phosphate apatite of Sr_{2+} cations or its insertion. (b) EXAFS modulations of the absorption coefficient as calculated f

The different structural hypotheses (figure 8a) regarding the localization of Sr^{2+} cations in bone which take into account the physicochemistry of biological apatite have been presented previously [52].

- hypothesis I : Sr^{2+} cations, only surrounded by oxygen atoms [49-50] are adsorbed at the
surface of collagen or apatite.

- hypothesis II : Sr^{2+} cations are engaged in the hydrated poorly crystalline apatite region present
at the surface of calcium phosphate nanocrystals.
- hypothesis III : Sr^{2+} cations are inside Ca phosphate nanocrystals on either crystallographic
site (CaI) or (CaII).

In order to assess these three different hypotheses, ab initio theoretical simulation of the XANES part of the absorption spectra and quantitative analyses taking into account multiple scattering processes of the EXAFS data were combined. In fact, EXAFS analysis seems to be the more efficient way to select a structural model (figure 8b). Data measured after the Sr K-edge are very similar to ones previously measured [49-54] in which Sr^{2+} cations are located inside the apatite crystal. Moreover, the complete set of experimental data collected on 17 physiological and pathological calcifications seems to indicate that there is no relationship between the nature of the calcification (physiological and pathological) and the adsorption mode of Sr^{2+} cations (simple adsorption or insertion).

6. Similar investigations on other beamlines

Research at the interface between physics, chemistry and medicine has been also performed on other beamlines implemented on other synchrotron facilities. Quite recently, Bohic *et al.* [55] have describe the possibilities offered by XRF and XAS in the biomedical field through very interesting examples of applications performed at the ESRF synchrotron-based microspectroscopy platform. We would like hereafter assess two examples in order to show the complexity as well as the wealth of such research.

A first example is given by Pt based drugs which as widely used in oncology [56]. To assess the electronic state as well as the local environment of Pt, XAS measurements are of great help. Indeed, the analysis of the XANES edge height provides information about the relative proportions of Pt(II) and Pt(IV) complexes [57] and the EXAFS data analysis gives important results on the surrounding environment of Pt [58-62]. Among the different breakthroughs, Serimaa *et al.* [63] describe for the first time the Pt−Pt partial radial distribution function of a biologically active Pt complex and explain the structure by a mixture model where the major components are mono- and binuclear Pt complexes.
More recently, Beret *et al.* [60] give evidence of a slight hydration structure around the Pt complex. A parallel, which can be established between the chemistry of Pt drugs and the one of Pt catalyst, has been already underlined [64].

Another example is given by physiological calcifications: major part of the investigations based on XAS measurements at the Ca K-edge are related to this physiological calcification [65-71]. Peters *et al.* [69] indicate that the size and morphology of the bone mineral particles are independent of the nature of the bone origin and that significant differences in the overall composition of the bone samples and in the carbonate content of the mineral phase exist. Similar results were obtained by Harries *et al.* [72]. Major information can be gathered also through XANES performed at the Ca L2,3- edges as these measurements are as well indicative of the local structure around Ca and can be performed on intracellular inclusions [73-76].

7. Conclusion and Perspectives

This presentation of investigations regarding pathological calcifications through different examples shows the importance of X-ray techniques using synchrotron radiation to achieve meaningful and effective analysis for medical applications. The few examples in the present paper show the crucial role of specific beamlines, as the DiffAbs beamline at SOLEIL, where it is possible to combine different techniques as XRF, XRD and XAS. Particularly, the imaging techniques are crucial and revealing a lot of information. Indeed, thanks to the rapid acquisition obtained by coupling the very great brightness of synchrotron source and the temporal performances of the new detectors (as hybrid pixel detectors for example) it is now possible to realize simultaneously large XRF and XRD maps to correlate elemental and structural information. Furthermore the recent development of "flyscan" method will strongly increase the acquisition performances, as it aims to realize acquisition in a continuous mode [77]. Another important instrument evolution on the DiffAbs beamline is linked to the current development of a new 2D hybrid pixel detector covering a large angular domain. Such instrument will allow to perform rapid XRD measurements but also will improve the possibility of diffraction-tomography and Pair Distribution Function (PDF) analyses.

Different technical aspect of the cited synchrotron techniques are not totally exploited and other existing techniques not yet developed in this field. For this reason, in addition to the already interesting results obtained, the scientific studies presented in this paper also open up new ideas for next scientific development in this field of research. For example, numerous major breakthroughs, innovative applications regarding medical nanotechnology are now available [78-80]. For example, nanometre-scale metallic clusters which have interesting natural bactericide and fungicide properties [81]. Next research in this domain typically require to focuses on theranostics, as defined by the combination of therapeutic and diagnostic agents on the very same single nanoparticle which has emerging as a very promising therapeutic paradigm. For such nanomaterials, opportunity to perform at the same time a characterization of nanometer scale cluster by XRD and of drug containing Pt by XAS will lead to major scientific breakthroughs regarding the deciphering of their interaction with tumors [81].

Acknowledgements

This work was supported by the Physics and Chemistry Institutes of CNRS and by contracts ANR-09-BLAN-0120-02 and ANR-12-BS08-0022. The authors are grateful to the Soleil Synchrotron Facility for beam time allocation and would like to very much thank the support group of SOLEIL for their help during experiment.

We also very much thank the following cited doctors for providing samples and useful discussions. Dr. I. Brocheriou, Prof. P. Jungers, Prof. B. Knebelman (Necker Hospital); Prof. P. Conort, Dr. P. Dorfmu ller and Dr. I. Tostivint (Lapitié Salpêtrière Hospital); Prof. D. Hannouche, Dr. E.A. Korng, Prof. F. Lioteì, Dr. Ch. Nguyen and Dr. Ch. Chappard (Lariboisière Hospital); Prof. J.P. Haymann, Dr. E. Letavernier, Dr. J. Rodes and Prof. O. Traxer from Tenon Hospital; Dr. X. Carpentier (Nice Hospital); Prof. M. Mathonnet (Limoges Hospital); Prof. P. Meria (St Louis Hospital); Prof. J.C. Williams (Department of Anatomy and Cell Biology, Indiana University School of Medicine, Indianapolis, Indiana, U.S.A.).

References

[1] D. Bazin, M. Daudon, Ch. Combes, Ch. Rey, Chemical Reviews 112 (2012) 5092.
[2] D. Bazin, M. Daudon, J. Phys. D, Applied Physics, 45 (2012) 383001.
[3] S. Hasnain, J. of Synchrotron Radiation, 14 (2007) 297.
[4] D. Bazin, X. Carpentier, O. Traxer, D. Thiaudière, A. Somogyi, S. Reguer, G. Waychunas, P. Jungers, M. Daudon, Journal of Synchrotron Radiation 15 (2008) 506.
[5] J. Monnier, S. Reguer, E. Foy, D. Testemale, F. Mirambet, M. Saheb, P. Dillmann, I. Guillot, Corrosion Science 78 (2014) 293.
[6] C. Mocuta, M.I. Richard, J. Fouet, S. Stanescu, A. Barbier, C. Guichet, O. Thomas, S. Hustache, A. Zozulya, D. Thiaudière, J. of Applied Crystallography 46(6) (2013) 1842.
[7] S. Djaziri, P.O. Renault, E. Le Bourhis, P. Goudeau, D. Faurie, G. Geandier, C. Mocuta, D. Thiaudiere, Journal of Applied Physics, 116 (2014) 093504.
[8] F.C. Breedveld, Rheumatology 43 (2004)
[9] E. Levy, A. Ferme, D. Perocheau, I. Bono, Rev. Rhum. Ed. Fr. 60 (1993) 63S.
[10] M. Watson, Pharm J. 259 (1997) 296.
[11] N. Arden, M.C. Nevitt, Best Pract Res. Clin Rheumatol 20(2006)3.
[12] D.J. Hunter, D.T. Felson, BMJ 332 (2006) 639.
[13] H.-K. Ea, Ch. Nguyen, D. Bazin, A. Bianchi, J. Guicheux, P. Reboul, M. Daudon, F. Lioté, Arthritis & Rheumatism 63 (2011) 10.
[14] Ch. Nguyen, H.-K. Ea, D. Bazin, M. Daudon, F. Lioté, Arthritis Rheum. 62 (2010) 2829.
[15] Ch. Nguyen, H.K. Ea, D. Thiaudière, S. Reguer, D.Hannouche, M. Daudon, F. Lioté, D. Bazin, J. of Synchrotron Radiation 18 (2011) 475.
[16] Ch. Nguyen, D. Bazin, M. Daudon, A. Chatron-Colliet, D. Hannouche, A. Bianchi, D. Côme, A. So, N. Busso, F. Lioté, H.-K. Ea, Arthritis Research & Therapy 15 (2013) R103
[17] H.-K. Ea, V. Chobaz, Ch. Nguyen, S. Nasi, P. van Lent, M. Daudon, A. Dessombz, D. Bazin, G. McCarthy, B. Jolles-Haeberli, A. Ives, D. Van Linthoudt, A. So, F. Lioté, N. Busso, PLoSONE 8 (2013) e57352.
[18] M. Daudon, Archives de Pédiatrie 20 (2013) 336.
[19] A. Randall, N. Engl. J. Med. 214 (1936) 234.
[20] A. Randall, Ann. Surg. 105 (1937) 1009.
[21] A.P. Evan, J. Lingeman, F.L. Coe, E. Worcester, Kidney Int. 69 (2006) 1313.
[22] M. Daudon, O. Traxer, P. Jungers, D. Bazin, Renal Stone Disease 900 (2007) 26.
[23] X. Carpentier, D. Bazin, Ch. Combes, A. Mazouyes, S. Rouzière, P.A. Albouy, E. Foy, M. Daudon, J. of Trace Elements in Medicine and Biology 25 (2011) 160.
[24] M. Daudon, D. Bazin, J. Phys.: Conf. Ser. 425 (2013) 022006.
[25] X. Carpentier, D. Bazin, P. Jungers, S. Reguer, D. Thiaudière, M. Daudon, J. of Synchrotron Radiation 17 (2010) 374.
[26] O. Johnell, J.A. Kanis, Osteoporos Int 17(2006) 1726.
[27] P.J. Meunier, C. Roux, E. Seeman, S. Ortolani, J.E. Badurski, T.D. Spector, J. Cannata, A. Balogh, E. Lemmel, S. Pors-Nielsen, R. Rizzoli, H.K. Genant,J. Reginster, N. Engl. J. Med. 350 (2004) 459.
[28] P.J. Marie, Curr. Opin. Pharmacol. 5 (2005) 633.
[29] B. Cortet, Curr. Osteoporos. Rep. 9 (2011) 25.
[30] A.L. Rossi, S. Moldovan, W. Querido, A. Rossi, J. Werckmann, O. Ersen, M. Farina Micron 56 (2014) 29.
[31] B. Busse, B. Jobke, M. Hahn, M. Priemel, M. Niecke, S. Seitz, J. Zustin, J. Semler, M. Amling, Acta Biomaterialia 6 (2010) 4513.
[32] Y.X. Zhang, Y.S. Wang, Y.P. Zhang, G.L. Zhang, Y.Y. Huang, W. He, NIM B 260 (2007) 178.
[33] G.R. Wohl, D.R. Chettle, A. Pejović-Milić, C. Druchok, C.E. Webber, J.D. Adachi, K.A. Beattie, Bone 52 (2013) 63.
[34] C. Li, O. Paris, S. Siegel, P. Roschger, E.P. Paschalis, K. Klaushofer, P. Fratzl, J. of Bone and Mineral Research 25 (2010) 968.
[35] A. Guinier, 1964 Théorie et Technique de la Radiocristallographie (Paris: Dunod)
[36] N.P. Camacho, S. Rinnerthaler, E.P. Paschalis, R. Mendelsohn, A.L. Boskey, P. Fratzl,

Bone 25 (1999) 287.
[37] P. Fratzl, H. Gupta, O. Paris, A. Valenta, P. Roschger, K. Klaushofer, Prog Colloid Polym Sci 130 (2005) 33.
[38] P. Fratzl, S. Schreiber, K. Klaushofer, Connect Tissue Res. 34 (1996) 247.
[39] A. Bigi, M. Falini, M. Gazzano, M. Roveri, Mater. Sci. Forum 278-281 (1988) 814.
[40] Z.Y. Li, W.M. Lam, C. Yang, B. Xu, G.X. Ni, S.A. Abbah, K.M.C Cheung, K.D.K. Luk, W.W. Lu, Biomaterials 28 (2007) 1452.
[41] A. Bigi, E. Boanini, C. Capuccini, M. Gazzano, Inorg. Chim. Acta 360 (2007) 1009.
[42] M.D. O'Donnel, Y. Fredholm, A. De Rouffignac, R.G. Hill, Acta Biomaterialia 4 (2008) 1455.
[43] R.V. Suganthi, K. Eayaraja, M.I. Ahymah Joshy, V.S. Chandra, E.K. Girija, S.N. Kalkura, Materials Science & Engineering in press
[44] A. Balerna, M. Bionducci, F. Falqui, G. Licheri, A. Meneghini, G. Navarra, M. Bettinelli, J. of Non-Crystalline Solids 232-234 (1998) 607.
[45] P. O'Day, M. Newville, P.S. Neuhoff, N. Sahai, S.A. Carroll, J. of Colloid and Interface Science 222 (2000) 184.
[46] D.M. Singer, S.B. Johnson, J.G. Catalano, F. Farges, G.E. Brown Jr, Geochimica et Cosmochimica Acta, 72 (2008) 5055.
[47] A.A. Finch, N. Allison, S.R. Sutton, M. Newville, Geochimica et Cosmochimica Acta, 67 (2003) 1197.
[48] N. Allison, A.A. Finch, M. Newville, S.R. Sutton, Geochimica et Cosmochimica Acta, 69 (2005) 3801.
[49] J. Terra, E. Rodrigues Dourado, J.-G. Eon, D.E. Ellis, G. Gonzalez, A.Malta Rossi, Physical Chemistry Chemical Physics 11 (2009) 568.
[50] Ch.G. Frankær, A.C. Raffalt, K. Stahl, Calcified Tissue International 94 (2014) 248.
[51] D. Bazin, M. Daudon, C. Chappard, J.J. Rehr, D. Thiaudière, S. Reguer, J. of Synchrotron Radiation 18 (2011) 912.
[52] D. Bazin, A. Dessombz, Ch. Nguyen, H.K. Ea, F. Lioté, J. Rehr, Ch. Chappard, S. Rouzière, D. Thiaudière, S. Reguer, M. Daudon, J. of Synchrotron Radiation 21 (2014) 136.
[53] I. Persson, M. Sandström, H. Yokoyama, M. Chaudhry, Z. Naturforsch. A 50 (1995) 21.
[54] M. Korbas, E. Rokita, W. Meyer-Klaucke, J. Ryczek, J. of Biological Inorganic Chemistry 9 (2004) 67.
[55] S. Bohic, M. Cotte, M. Salomé, B. Fayard, M. Kuehbacher, P. Cloetens, G. Martinez-Criado, R. Tucoulou, J. Susini, Journal of Structural Biology 177 (2012) 248.
[56] A. V. Klein, T. W. Hambley, Chem. Rev. 109 (2009) 4911.
[57] M.D. Hall, G.J. Foran, M. Zhang, Ph.J. Beale, T.W. Hambley. J. of American Chemical Society 125 (2003) 7524.
[58] D. Bouvet, A. Michalowicz, S. Crauste-Manciet, D. Brossard, K. Provost. Inorganic Chemistry 45 (2006) 3393.
[59] D. Bouvet, A. Michalowicz, S. Crauste-Manciet, E. Curis, I. Nicolis, L. Olivi, G. Vlaic, D. Brossard,K. Provost, J. of Synchrotron Radiation, 13 (2006) 477.
[60] E.C. Beret, K. Provost, D. Müller, E. Sánchez Marcos, J. Phys. Chem. B 113 (2009) 12343.
[61] K. Provost, D. Bouvet-Muller, S. Crauste-Manciet, J. Moscovici, L. Olivi, G. Vlaic, A. Michalowicz, Biochimie. 91(2009)1301.
[62] K. Provost, E C Beret, D Bouvet Muller, A Michalowicz, E Sánchez Marcos, The Journal of Chemical Physics 138 (2013) 084303.
[63] R. Serimaa, V. Eteläniemi, T. Laitalainen, A. Bienenstock, S. Vahvaselkä, T. Paakkari, Inorg. Chem. 36 (1997) 5574.
[64] D. Bazin, C. R. Chimie 17 (2014) 615.
[65] J.E. Harries, D.W.L. Hukins, C. Holt, S.S. Hasnain, J. Cryst. Growth, 84 (1987) 563.
[66] D. Eichert, M. Salomé, M. Banu, J. Susini, Ch. Rey, Spectrochimica Acta B 60 (2005) 850.
[67] K. Asokan, J.C. Jan, J.W. Chiou, W.F. Pong, P. K. Tseng, I.N. Lin, J. of Synchrotron Radiation, 8 (2001) 839.
[68] R.M. Miller, D.W.L. Hukins, S.S. Hasnain, P. Lagarde, Biochemical and Biophysical Research Communications 99 (1981) 102.
[69] F. Peters, K. Schwarz, M. Epple, Thermochimica Acta, 361 (2000) 131.

[70] Ch.G. Frankær, A.Ch. Raffalt, K. Stahl, Calcified Tissue International 94 (2014) 248.
[71] M. Korbas, E. Rokita, W. Meyer-Klaucke, J. Ryczek,
J. of Biological Inorganic Chemistry 9 (2004) 67.
[72] J.E. Harries, D.W.L. Hukins, S.S. Hasnain, Calcif. Tissue Int. 43 (1988) 250.
[73] M.E. Fleet, X. Liu, American Mineralogist 94 (2009) 1235.
[74] E. Couradeau, K. Benzerara, E. Gérard, D. Moreira, S. Bernard, G.E. Brown Jr.,
P. López-García, Science 336 (2012) 459.
[75] K. Benzerara, T.H. Yoon, T. Tyliszczak, B. Constantz, A.M. Spormann, G.E. Brown,
Geobiology 2 (2004) 249.
[76] K. Benzerara, N. Menguy, M. Obst, J. Stolarski, M. Mazur, T. Tylisczak, G.E. Brown,
A. Meibom, Ultramicroscopy, 111 (2011) 1268.
[77] K. Medjoubi, N. Leclercq, F. Langlois, A. Buteau, S. Lé, S. Poirier, P. Mercère, M. Sforna,
C.M. Kewish, C. M., and A. Somogyi, J. of Synchrotron Radiation 20(2), (2013), 293
[78] S.M. Janib, A.S. Moses, J.A. MacKay, Adv. Drug Deliv. Rev. 62 (2010) 1052.
[79] J. Xie, S. Lee, X. Chen, Adv. Drug. Deliv. Rev. 62 (2010) 1064.
[80] S. Harrisson, J. Nicolas, A. Maksimenko, D.T. Bui, J. Mougin, P. Couvreur,
Angewandte Chemie 125 (2013) 1722.
[81] L.G. Bach, R. Islam, T.-S. Vo, S.-K. Kim, K.T. Lim,
J. of Colloid and Interface Science 394 (2013) 132.